

# Late Pleistocene emergence of an anthropogenic fire regime in Australia's tropical savannahs

Received: 12 March 2023

Accepted: 26 January 2024

Published online: 11 March 2024

 Check for updates

Michael I. Bird <sup>1,2</sup>✉, Michael Brand<sup>1,2</sup>, Rainy Comley <sup>1,2</sup>, Xiao Fu <sup>3</sup>,  
Xennephone Hadeen<sup>1,2</sup>, Zenobia Jacobs <sup>2,4</sup>, Cassandra Rowe <sup>1,2</sup>,  
Christopher M. Wurster<sup>1,2,6</sup>, Costijn Zwart <sup>1</sup> & Corey J. A. Bradshaw <sup>2,5</sup>

At the time of European arrival on the Australian continent, sophisticated Indigenous societies practiced land management across Australia's extensive tropical savannahs. Fire was one of the main tools people used to manipulate fuel loads and connectivity to reduce uncontrolled wildfire, maintain vegetation structure and enhance biodiversity. When this alteration of a 'natural' fire regime to a human-dominated fire regime occurred is not known. Here we assessed fire incidence and intensity over the past 150,000 years through a continuous lacustrine record by comparing the accumulation rates of micro-charcoal and stable polycyclic aromatic hydrocarbon that form during the combustion of vegetation. We also compared grass (mainly C<sub>4</sub>) pollen as a percentage of total dryland pollen with the carbon isotope composition of the stable polycyclic aromatic hydrocarbon. We established with high statistical certainty that a change in fire regime occurred at least 11,000 years ago from less-frequent, more-intense fires to more-frequent, less-intense fires. This change marked the overprinting of a largely natural fire regime by one at least modulated by Indigenous management. Our findings demonstrate that human fire use has modified fire regimes throughout the Holocene and also show how people have managed the potential for the type of high-intensity fires that are likely to increase in the future.

Wildfire currently burns  $3.94\text{--}5.19 \times 10^6$  km<sup>2</sup> of land annually<sup>1</sup>. Fire has always modified the terrestrial carbon cycle, ecosystem function and biodiversity, from the tropics to high latitudes<sup>2,3</sup>. The incidence and severity of wildfires around the world are increasingly affected by human endeavour, including associated climate change, with catastrophic impacts of severe fires now occurring in many parts of the world<sup>4–7</sup>.

Fire is also one of the earliest tools appropriated by humans<sup>2</sup>, with the earliest deliberate use of fire by hominins dating from ~1 million years ago<sup>8</sup>. Habitual use of fire potentially allowed manipulation of fire frequency and fire seasonality from as early as 250 ka to 350 ka (refs. 9,10). As human populations grew, and developed both agriculture and pastoralism into the Holocene, our species also achieved an increasing measure of control over fuel loads and

<sup>1</sup>College of Science and Engineering, James Cook University, Cairns, Queensland, Australia. <sup>2</sup>Australian Research Council Centre of Excellence of Australian Biodiversity and Heritage, Wollongong, Australia. <sup>3</sup>Key Laboratory of Geoscience Big Data and Deep Resource of Zhejiang Province, School of Earth Sciences, Zhejiang University, Hangzhou, China. <sup>4</sup>Centre for Archaeological Science, School of Earth, Atmospheric and Life Sciences, University of Wollongong, Wollongong, New South Wales, Australia. <sup>5</sup>Global Ecology | Partuyarta Ngadluku Wardli Kuu, College of Science and Engineering, Flinders University, Adelaide, South Australia, Australia. <sup>6</sup>Present address: Isotracer NZ Ltd, Dunedin, New Zealand. ✉e-mail: [michael.bird@jcu.edu.au](mailto:michael.bird@jcu.edu.au)



**Fig. 1 | Location of Girraween Lagoon.** The coastline of modern Australia is shown by the solid white line on the landmass at the maximum extent of lower sea level during the Last Glacial Maximum. **a**, Modern vegetation. **b**, Satellite image of the site. The other locations are mentioned in the text, and the modern southern limit of the savanna biome is shown as a dashed white line. Map data from Google, Maxar Technologies.

fuel connectivity, and therefore fire regime—that is, fire incidence and intensity<sup>9</sup>.

Humans have modified both modern landscapes and patterns of biodiversity that were considered ‘natural’ for millennia before the transformations that have occurred since the Industrial Revolution<sup>11–14</sup>. Fire was one of several tools used by pre-industrial societies to modify and manage land and resources<sup>9</sup>. The cessation of Indigenous fire management in many parts of the world has contributed to biodiversity decline and, through a build-up of connected fuel loads, an increase in catastrophic fires<sup>5,14–16</sup>.

There is abundant evidence for human use and manipulation of their environment extending back at least tens of millennia<sup>17</sup>; however, separating anthropogenic and climatic impacts on fire regime in prehistory is challenging<sup>2,18,19</sup>. Clear and diverse human impacts, including those on fire regime, are uncommon in the early Holocene<sup>20</sup>, but become progressively more common from the mid-Holocene in regions where societies transitioned to agriculture, pastoralism and urbanization<sup>21</sup>.

Human manipulation of fire regimes in the large areas occupied by low-density hunter-gatherer populations has been difficult to identify<sup>2,19</sup>. Where detection has been claimed, the evidence is generally derived from the appearance of, or abrupt increase in, the abundance of micro-charcoal particles in sedimentary records—often in conjunction with pollen evidence of the modification of local vegetation. Most studies claim the detection of a hunter-gatherer influence on fire from the mid- to late Holocene in Australia<sup>22</sup>, southern Africa<sup>23</sup> and North America<sup>24</sup>. It is not yet known whether the many well-documented impacts of Indigenous fire management on many aspects of biodiversity could have been developed over only a few millennia<sup>12,19</sup>.

Detecting prehistoric human influence on fire regime is especially problematic in tropical savannas, where fire has always had a short (generally sub-decadal) return interval and vegetation is adapted to fire<sup>25</sup>. Charcoal is therefore continuously detectable in savanna environmental records regardless of the source of ignition. In Australia, as elsewhere, anthropogenic climate change exacerbated by the cessation of Indigenous fire management is driving a trend towards more extreme fires<sup>14–16,26</sup>. While the catastrophic fires in southern Australia in 2019–2020 received much attention<sup>5,6,27</sup>, most fires occur in the tropical savannas of northern Australia (70% of total burnt area 1997–2001<sup>28</sup>). While fire is a natural driver of ecosystem dynamics in savannas, the cessation of Indigenous land management over much of northern Australia following European arrival<sup>11,19,29,30</sup> has changed vegetation structure<sup>31,32</sup> and fuel characteristics<sup>33,34</sup>. This has decreased biodiversity and altered the carbon balance<sup>19,29,35–37</sup>.

Fire has been shaping Australia’s terrestrial ecosystems for millions of years<sup>38</sup>. Humans arrived on the continent ~65,000 years ago<sup>39</sup>, radiating across the continent over the next 5,000 to 10,000 years (refs. 40,41). The prevalence of Indigenous use of fire through ‘firestick farming’<sup>42</sup> is now thought to have been essential to maintaining the landscapes and biodiversity observed across northern Australia and considered natural at European arrival<sup>11,29,30</sup>. An early claim of evidence of human impact identified through an abrupt increase in micro-charcoal abundance 40,000 years ago at Lynch’s Crater in north-eastern Australia<sup>43</sup> has not been supported by subsequent meta-analyses of compilations of larger sets of charcoal records around the country<sup>44,45</sup>. However, few of these records are long enough to assess the characteristics of a natural fire regime. We used multiple fire and climate indicators in a continuous savanna sediment record spanning the past 150,000 years to identify whether (and if so, when) Indigenous fire management became a dominant control on fire regime and ecosystem dynamics in the savannas of northern Australia.

## A 150-ka record of climate and vegetation in northern Australia

Girraween lagoon (12° 31′ 3.6″ S, 131° 04′ 50.7″ E, 25 m above sea level; Fig. 1) is a perennial waterbody located on the outskirts of Darwin, Northern Territory, Australia. The climate is monsoonal with a mean annual regional rainfall of 1,731 mm (Bureau of Meteorology Station 014015, Darwin Airport), 90% of which falls between November and April. The modern vegetation around the lagoon is *Eucalyptus*-dominated tropical open-forest savanna and/or savanna woodland (dominant overstorey: *Eucalyptus tetradonta*, *Eucalyptus miniata* and *Corymbia polycarpa*) with a grassy understorey. The modern environment and evolution of the lagoon since 26.6 ka has been described in detail<sup>46,47</sup>.

The lagoon formed following collapse into a sinkhole and has been permanently wet since that time. During dry periods, the waterbody was restricted to the sinkhole itself (~0.01 km<sup>2</sup>); during wet periods (as today) the surface area expands across a shallow depression to an area of 0.45 km<sup>2</sup> (Fig. 1). The site is 200 km west of the earliest archaeological site of Madjedbebe<sup>39</sup> and, as a permanent water source, the 0.92 km<sup>2</sup> catchment is likely to have had some human presence for ~65,000 years.

A 19.4 m core was collected using a floating platform with hydraulic coring rig in 4.5 m of water, with 235 samples taken at 5–10 cm intervals. The record is composed of alternating peats that formed during wet periods with high lake levels, and clays deposited during dry periods with low water levels. The chronology for the record is provided by 12 radiocarbon<sup>46,47</sup> dates and 24 optically stimulated luminescence dates (Supplementary Table 1).

Peaks in the total organic carbon (TOC) content corresponding to high lake levels occur mainly in Marine Isotope Stages (MIS) 1 and 5, with the largest of these (>15% TOC) relating to insolation maxima in the region (Fig. 2a). These reflect wet monsoonal conditions similar to today. Rainfall at the site is also modulated by the distance to the coast<sup>47</sup>—the low offshore bathymetric gradient means that the coast retreats by up to 320 km during glacial periods. Smaller peaks in TOC (<10%), indicative of wet conditions, are related to times of higher sea level and/or times of higher insolation (Fig. 2a). From MIS 4 to MIS 2 there was an extended period of uniformly low lake level regardless of insolation (<2% TOC). This period is due at least in part to the distance to the coast being 150–320 km, because rainfall decreases away from coasts in monsoonal climates downwind of the moisture-source region, becoming progressively drier as previous rainout occurs<sup>48</sup>. It is also due to comparatively low insolation over this period that weakened monsoon intensity<sup>49</sup> (Fig. 2a).

## A 150 ka record of fire regime in northern Australia

We used three measures of fire derived from the Girraween lagoon record: (1) micro-charcoal particle accumulation rate (PAR<sub>char</sub>; Fig. 2b), the most commonly applied indicator of fire, for which

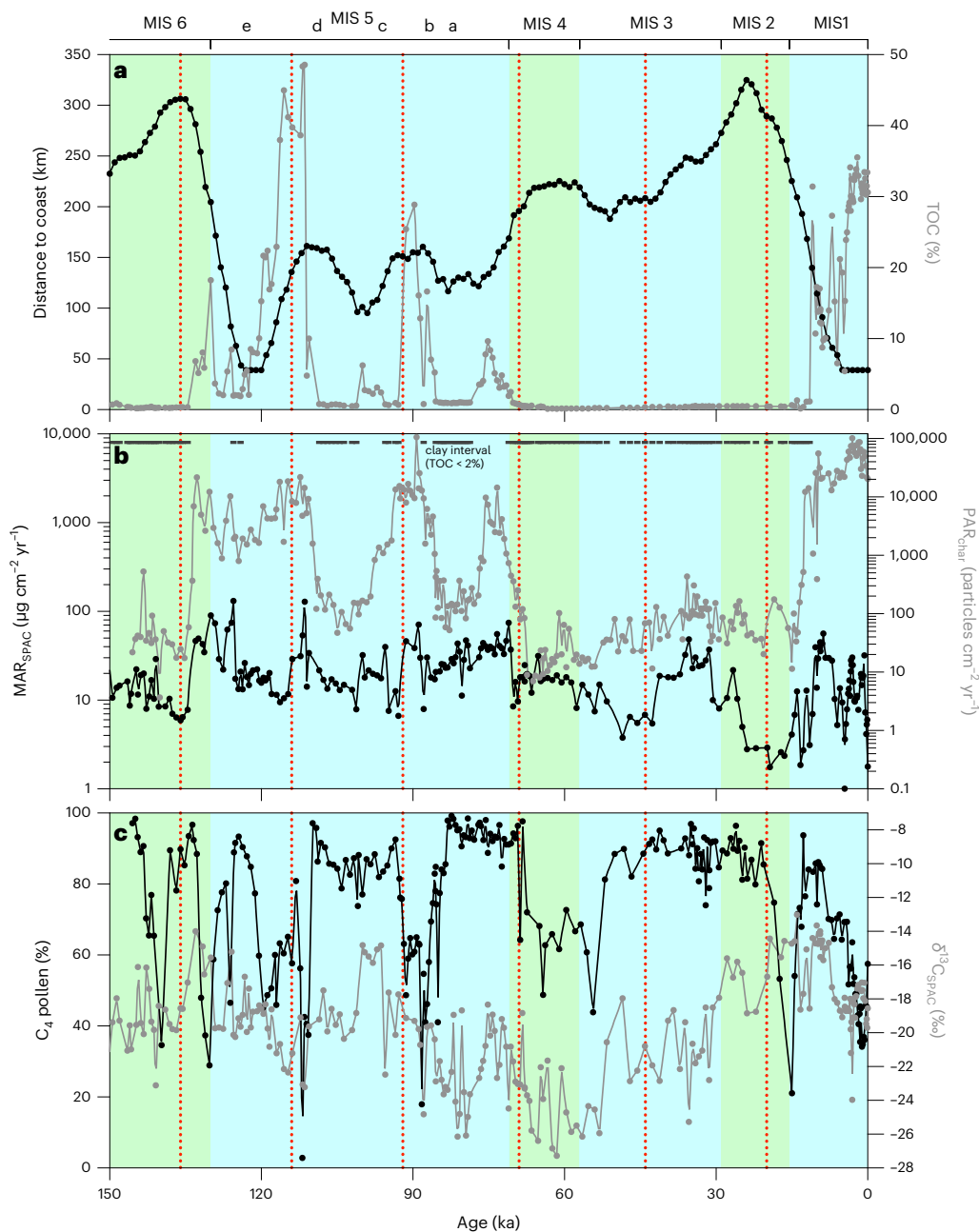


**Fig. 2 | 150 ka record of environmental change at Girraween Lagoon. a.** TOC content (right y axis) and the distance to the coast (left y axis) through time. The distance to the coast was calculated using the average of the bathymetry on transects north and northwest from the coast adjacent to Girraween Lagoon to the continental shelf edge and the LS16 sea level curve<sup>73</sup>. **b.**  $PAR_{char}$  (right y axis) and  $MAR_{SPAC}$  (left y axis) both on a logarithmic (base 10) scale (Supplementary Fig. 2 shows the two time series on a linear scale). **c.** Grass pollen as a percentage

of total dryland pollen (left y axis) and  $\delta^{13}C_{SPAC}$  (right y axis). Measured values (dots) do not always correspond exactly to 250 yr interpolated values (Methods). The alternating background colours correspond to approximate MIS durations, with the peaks of MIS 5 substages also identified (a–e)<sup>73</sup>. Wet-season (December to March) insolation peaks at 15° S occur at 136, 114, 92, 70, 45, 19 and -0 ka (vertical red dotted lines, 0 ka not shown; see Supplementary Fig. 2 for insolation curves).

higher accumulation rates indicate a higher incidence of fire<sup>44</sup>; (2) the mass accumulation rate (MAR) of stable polycyclic aromatic carbon (SPAC) by hydrogen pyrolysis ( $MAR_{SPAC}$ ; Fig. 2b). This is a geochemical measure of the proportion of carbon in condensed (>7) aromatic rings in the char, indicating temperature of formation<sup>22,50–52</sup>. The combination of these two measures allows inference of relative fire intensity, because the proportion of SPAC in char increases as a function of the temperature at which it is produced. Thus, higher-intensity fires will produce char containing abundant SPAC, while lower-intensity fires will produce char with little SPAC<sup>22,50–52</sup>. (3) We also measured the  $\delta^{13}C$  of the SPAC ( $\delta^{13}C_{SPAC}$ ; Fig. 2c), which provides a relative measure of the

proportion of grass-derived (mainly  $C_4$ ) relative to tree/shrub-derived (exclusively  $C_3$ ) biomass that is not combusted, but is instead preserved as SPAC<sup>50–52</sup>. The  $\delta^{13}C_{SPAC}$  is broadly determined by vegetation, and therefore climate, but is also modified because high-intensity fires more fully combust fine (grassy) fuels<sup>33,50</sup>, leading to a relative increase in larger woody ( $C_3$ )-derived biomass preserved in the charcoal and therefore, a lower  $\delta^{13}C_{SPAC}$  compared with the  $\delta^{13}C$  of the biomass.

$PAR_{char}$  (Fig. 2b) varies by five orders of magnitude (4–105,400 particles  $cm^{-2} yr^{-1}$ ); it was high during periods of wetter climate (defined herein by high TOC and a generally lower grass pollen contribution to total dryland pollen; % $C_4$  pollen) and low during drier intervals

(low TOC and high %C<sub>4</sub> pollen). The apparently low PAR<sub>char</sub> in the clay-rich sediments that dominate during dry periods (<2% TOC) are an artefact of char–clay mineral interactions<sup>53,54</sup>. These lead to charcoal particles in the clay sediments, particularly fragile grass-derived charcoal, being comminuted to below the minimum size for counting (<10 µm; Methods) during laboratory disaggregation of the sediment, however gentle. This means that PAR<sub>char</sub> is only a reliable indicator of relative fire incidence during intervals of higher TOC. The mean PAR<sub>char</sub> through the Holocene is 42,200 particles cm<sup>-2</sup> yr<sup>-1</sup>, more than double the means for the previous two highest multi-millennial peaks in accumulations in the past 150 ka (16,700 and 10,500 particles cm<sup>-2</sup> yr<sup>-1</sup>), both of which occur at times of high insolation near 114 and 92 ka, similar to the Holocene (Fig. 2b and Supplementary Fig. 2).

As a geochemical measure, MAR<sub>SPAC</sub> (Fig. 2b and Supplementary Fig. 2) is insensitive to clay content and is present throughout the record. Accumulation rates range over three orders of magnitude (1–131 mg cm<sup>-2</sup> yr<sup>-1</sup>); rates are most consistently high through interglacial MIS 5 (mean MAR<sub>SPAC</sub> = 30.2 mg cm<sup>-2</sup> yr<sup>-1</sup>) and consistently low in glacial stage MIS 2 (mean MAR<sub>SPAC</sub> = 6.5 mg cm<sup>-2</sup> yr<sup>-1</sup>; Fig. 2b and Supplementary Fig. 2).

Tree–grass balance as a measure of savannah response to changing rainfall, rainfall distribution and potentially Indigenous management (percentage of C<sub>4</sub> pollen; Fig. 2c) ranges widely and varies substantially over centennial timeframes. The major wetter periods are generally characterized by 30–50% (minimum 2.8%) C<sub>4</sub> pollen, indicating a more wooded savannah. During drier periods, C<sub>4</sub> pollen often comprised >80% (maximum 99.2%) of the total dryland pollen, which is suggestive of an open, grassy savannah. The δ<sup>13</sup>C<sub>SPAC</sub> (Fig. 2c) also ranged widely from –27.3 to –13.0‰ and exhibited only limited similarity at the broadest scale to the pollen record.

## Separating anthropogenic from natural fire regime

The vegetation structure of tropical savannahs is influenced by both fire incidence and intensity, which in turn vary with climate, climate variability, land management and the frequency of ignition<sup>31,55</sup>. Tree cover responds to changes in fire regime on a decadal timescale<sup>32</sup>. In Australia's tropical savannahs, fire regime is influenced by precipitation and precipitation variability<sup>56,57</sup> in combination with seasonal temperature changes<sup>57</sup>. Land management affects grass biomass<sup>58</sup>, and the flammability of both grass biomass<sup>59,60</sup> and litter<sup>60,61</sup>. Higher fuel loads produce hotter fires<sup>34</sup>, so the time since the last fire affects intensity<sup>62</sup>. Fire size and intensity increase in the late dry season<sup>63</sup>, while early dry-season fires have a lower intensity<sup>64</sup>.

The attributes of an Indigenous fire regime in northern Australia are well documented. They include the use of frequent burning (1–3 yr return interval) of small areas (hectares to tens of hectares) to maintain low fuel loads and connectivity beginning in, but not confined to, the early dry season<sup>30,36,65,66</sup>. These are low-intensity fires limited to the ground layer, thereby reducing the risk of large, high-intensity fires while promoting a mosaic of vegetation and attendant biodiversity. This regime produces a low proportion of SPAC in the char created and a relatively high δ<sup>13</sup>C<sub>SPAC</sub>, because a larger component of grassy fuel is more likely to be preserved as charcoal instead of being fully combusted.

The characteristics of a natural fire regime in Australia's tropical savannahs cannot be observed directly today, but can be inferred on the basis of lightning being the only source of ignition, and climate being the dominant control of fire regime. The average modern density of lightning strikes is 1.21 km<sup>-2</sup> yr<sup>-1</sup>, with more lightning striking grasslands than wooded vegetation classes<sup>67</sup>. Almost no strikes occur in the region from April to September (early dry season), but they peak in November and December during the transition to wet season conditions. With considerably fewer sources of ignition, and successful ignitions likely to result in fires concentrated in the late dry season<sup>68</sup>,

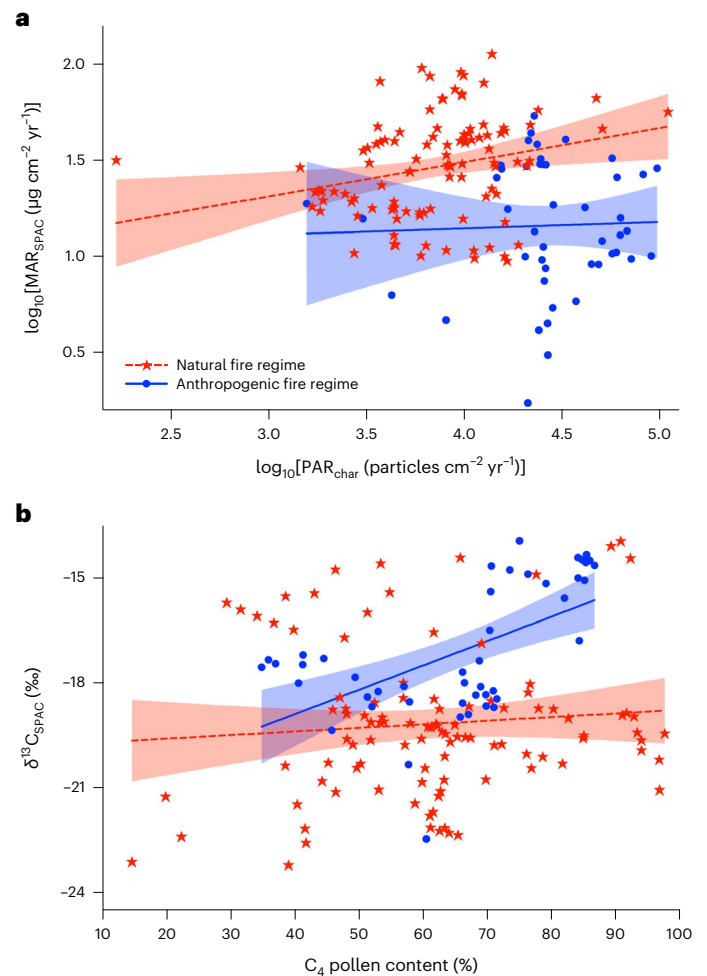


**Fig. 3 | Relationships between fire and vegetation indices at Gिरraween lagoon. a**, Relationship between MAR<sub>SPAC</sub> and PAR<sub>char</sub>. We hypothesized a more pronounced positive relationship under the pre-human natural fire regime than under the lower-intensity fires present in the anthropogenic fire regime. **b**, Relationship between the percentage of C<sub>4</sub> pollen and δ<sup>13</sup>C<sub>SPAC</sub>. We hypothesized a more pronounced positive relationship under the lower-intensity fires present in the anthropogenic fire regime than under the pre-human natural fire regime. In both cases, the relationships pertain only to periods where the TOC is >5.1%, and the hypothesized temporal split between the natural and anthropogenic periods is 30 ka. Red dashed lines indicate the best-fit relationships with uncertainty for periods dominated by a natural fire regime, and solid blue lines indicate best-fit relationships with uncertainty during periods dominated by anthropogenic fire regimes. We provide the relationship for all samples in Supplementary Fig. 1.

a natural fire regime probably has fewer fires. Those that do occur are higher intensity due to greater, more fully cured fuel loads, and burn larger areas due to greater fuel connectivity. A higher-intensity fire will more completely combust biomass, particularly fine fuels such as grass and litter, thereby producing less char<sup>50,69</sup> and a higher proportion of SPAC in that char. A natural fire regime will produce relatively lower δ<sup>13</sup>C<sub>SPAC</sub> from the higher preservation potential of coarse, woody fuels relative to fine, grassy fuels—a phenomenon known as the savannah isotope disequilibrium effect<sup>50</sup>.

We therefore hypothesize that a natural (more-intense) fire regime will be identifiable by: (1) a relatively lower PAR<sub>char</sub> containing relatively more SPAC than under an anthropogenic fire regime; and (2) a lower δ<sup>13</sup>C<sub>SPAC</sub> relative to the δ<sup>13</sup>C of the biomass as measured by the percentage of grass pollen in the total dryland pollen count. An anthropogenic (less-intense) fire regime will be identifiable by: (1) a relatively higher PAR<sub>char</sub> containing relatively less SPAC than under a natural fire regime;

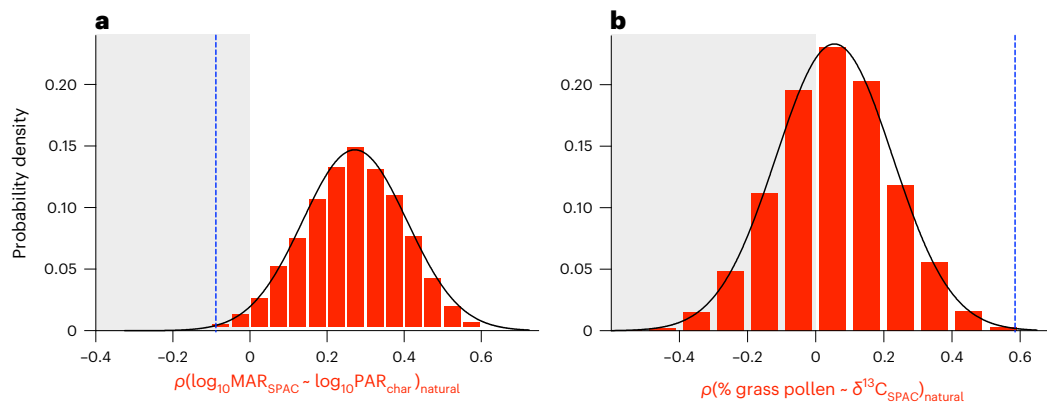


**Fig. 4 | Histograms of Spearman's correlation coefficient for fire and vegetation indices at Girraween lagoon. a**, Relationship between  $MAR_{SPAC}$  and  $PAR_{CHAR}$  resampled for the natural fire regime (>30 ka; red bars) relative to the observed Spearman's correlation coefficient ( $\rho$ ) for the anthropogenic fire regime (<30 ka; blue vertical dashed line). **b**, Relationship between the percentage of  $C_4$  pollen and  $\delta^{13}C_{SPAC}$  resampled for the natural fire regime (>30 ka; red bars) relative to the observed Spearman's  $\rho$  for the anthropogenic

fire regime (<30 ka; blue vertical dashed line). The relationships pertain only to samples where the TOC is >5.1%. The probabilities of generating the result randomly are 0.0071 (a) and <0.0002 (b) for this combination of thresholds. The regions shaded grey indicate  $\rho < 0.05$ . In both panels, x axes indicate the binned value of  $\rho$  for the relationship (indicated by -) between each variable under the natural fire regime across all iterations. Solid black lines indicate probability density function describing the Gaussian shape of each histogram.

and (2) a higher  $\delta^{13}C_{SPAC}$  relative to the  $\delta^{13}C$  of the biomass as inferred from the percentage of  $C_4$  pollen. Under both natural and anthropogenic fire regimes, micro-charcoal is dispersed by wind and water<sup>70,71</sup>, with grass-derived char being dispersed more widely than char derived from woody materials<sup>71</sup>. This difference in dispersal potential means that charcoal (and pollen) in terrestrial records such as Girraween, close to the area being burnt, tends to be biased towards larger, less aerodynamic size classes, often wood-derived charcoal. In contrast, marine records remote from sites of burning will be biased towards smaller, more aerodynamic size classes, often grass-derived charcoal<sup>71</sup>.

The combined records (Fig. 2) can be assessed from the perspective that the record before 65 ka, and for some unknown period after, must reflect a natural fire regime. There are clear qualitative differences. Comparing the glacial stages, for example, the  $MAR_{SPAC}$  in MIS 2 (post-human arrival) was one-third of that in MIS 6 (pre-human arrival). Comparing interglacial stages,  $PAR_{CHAR}$  in MIS 1 (post-human arrival) was more than double that observed at any time in MIS 5 before human arrival (Fig. 2b and Supplementary Fig. 2).

There is considerable intersample variation throughout the record, and it is of course also possible that low-intensity fires always resulted stochastically from lightning ignitions, and that climate extremes might promote periods of intense fires. We therefore tested for statistical dissimilarity in the records (Methods) using 30 ka as the arbitrary time after which there was a transition to an identifiable anthropogenic fire regime. We compared the two measures of fire ( $PAR_{CHAR}$  and  $MAR_{SPAC}$ ) and the two measures of vegetation (percentage of  $C_4$  pollen and  $\delta^{13}C_{SPAC}$ ). To control for the impact of the particle accumulation rate of micro-charcoal in the high clay content in parts of the core, we tested whether the choice of a TOC threshold modified our results (Methods). When TOC is >5.1%, the attributes of the record after 30 ka are different to the natural fire regime in place for the preceding 120 ka and consistent with the establishment of an anthropogenic fire regime at some time after 30 ka (Figs. 3 and 4). The decline in time-series length (sample size  $n$ ) for the youngest (anthropogenic fire-regime) period does not affect variance in any of the measures until <3 ka (Supplementary Fig. 3), demonstrating that the shift from natural to anthropogenic fire regimes is not an artefact of diminishing statistical power.

## Evolving fire regimes into the Holocene

The temporal depth of the multiple proxies in the Girraween record enables us to determine the attributes of a natural fire regime as expressed

in the proxies before human arrival. This then allows us to attribute influence on fire regime in the period younger than -11 ka to human agency with statistical confidence, because the probabilities of a randomly generated difference between the natural versus anthropogenic fire regime using all indicators quickly rise to high values (>0.05) when TOC exceeds 2% (Fig. 5a) and after 11 ka (Fig. 5b). It is unlikely that any anthropogenic influence on fire regime was imposed instantaneously, so some measure of control was probably exercised before 11 ka. The high  $\delta^{13}C_{SPAC}$  around 15 ka when the percentage of  $C_4$  pollen was low, as well as the low  $MAR_{SPAC}$  in glacial MIS 2 compared with glacial MIS 6, provides qualitative evidence that this was the case. A trend towards increased  $\delta^{13}C_{SPAC}$  (Fig. 2c) over a period when vegetation was stable that began before -30 ka could also indicate an early, progressive implementation of Indigenous fire management. However, the clay-rich sediments during these periods make the  $PAR_{CHAR}$  unsuitable for direct comparison to  $MAR_{SPAC}$ .

It is possible that anthropogenic influence increased progressively through the post-glacial period of sea-level rise following the end of MIS 2, with small human populations in the interior of Sahul<sup>45</sup> in glacial MIS 2 limiting peoples' ability to affect fire regime. It is clear that as population densities increased in the Holocene<sup>45</sup>, the savannahs around Girraween Lagoon, and by implication, across northern Australia, were modified from their natural state. This change might have been initiated in post-glacial times by monsoon reactivation, leading to the return of mesic savannahs and higher fuel loads than had been seen in the Girraween Lagoon area since human arrival.

While climate ultimately dominates the variability in fire regime, Indigenous management of fire observed ethnographically across northern Australia was firmly in place from the earliest Holocene. It is plausible that Indigenous fire management was developed over millennia in the wetter coastal regions on the now-flooded Sahul shelf, introduced to the Girraween lagoon region as populations retreated landwards in the face of post-glacial sea-level rise (Fig. 2a). It seems unlikely that the Australian case is unique, and low-density hunter-gatherer populations in other parts of the world might similarly have established control over fire regimes earlier than is currently recognized.

Our results suggest that the mesic savannahs at Girraween Lagoon were established over several millennia under a fire regime influenced by Indigenous fire management from at least the early Holocene.

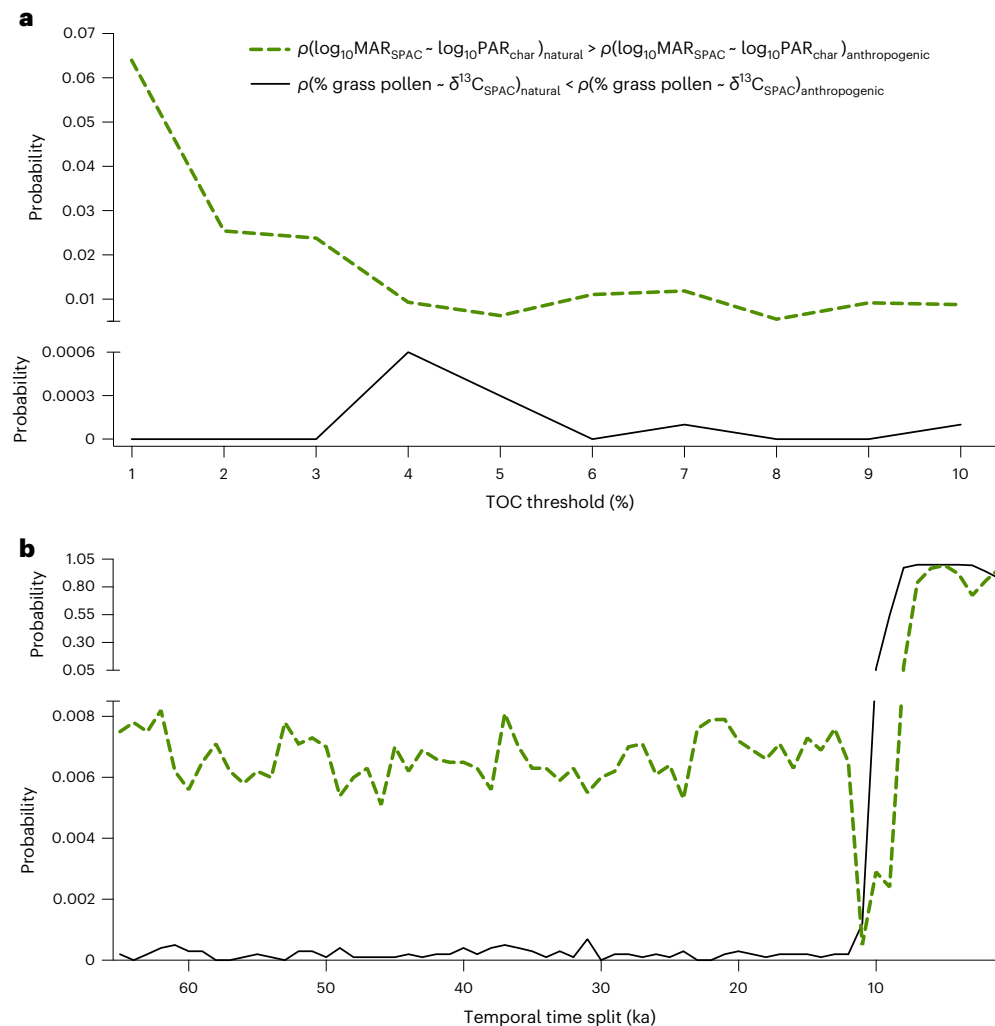


**Fig. 5 | Sensitivity of hypothesis to fire and vegetation indices at Gिरraween lagoon. a, b.** Sensitivity to variation in the choice of the TOC threshold (a; temporal split constant at 30 ka) and the temporal split defining the change from natural to anthropogenic fire regimes (TOC threshold constant at >2%). The probability that the relationship measured as Spearman's  $\rho$  between  $MAR_{SPAC}$  and  $PAR_{CHAR}$  is greater for the natural fire regime than the anthropogenic fire

regime is shown by the green dashed line. The probability that the relationship measured as Spearman's  $\rho$  between the percentage of  $C_4$  pollen and  $\delta^{13}C_{SPAC}$  is greater for the anthropogenic fire regime than the natural fire regime is shown by the solid black line. Both hypothesis test outcomes are insensitive to the choice of either threshold at TOC thresholds >2% and temporal splits older than 10 ka. See the Methods for explanation of our approach.

This fire regime was fundamentally different to previous times when mesic savannahs were present at the site during MIS 5. It is therefore unsurprising that the rapid change to a European fire regime, with an increased incidence of larger, more-intense, late dry-season fires reminiscent of the natural fire regime has massively altered biodiversity<sup>19,35</sup> and increased greenhouse gas emissions<sup>65</sup>. Reversing these trends in Australia's tropical savannahs requires the re-implementation of an Indigenous fire regime<sup>30,36</sup>, with additional benefits including an increase over time in tree biomass of  $-0.11$  t dry matter  $ha^{-1}$  (ref. 72). By implication, the reintroduction of Indigenous land-management strategies in other parts of the world could assist in mitigating the impact of catastrophic fires, and increase carbon sequestration in the future<sup>14,15</sup>.

### Online content

Any methods, additional references, Nature Portfolio reporting summaries, source data, extended data, supplementary information, acknowledgements, peer review information; details of author contributions and competing interests; and statements of data and code availability are available at <https://doi.org/10.1038/s41561-024-01388-3>.

### References

- Lizundia-Loiola, J., Otón, G., Ramo, R. & Chuvieco, E. A spatio-temporal active-fire clustering approach for global burned area mapping at 250 m from MODIS data. *Remote Sens. Environ.* **236**, 11493 (2020).
- Bowman, D. M. et al. The human dimension of fire regimes on Earth. *J. Biogeogr.* **38**, 2223–2236 (2011).
- Bird, M. I., Wynn, J. G., Saiz, G., Wurster, C. M. & McBeath, A. The pyrogenic carbon cycle. *Annu. Rev. Earth Planet. Sci.* **43**, 273–298 (2015).
- Abatzoglou, J. T., Williams, A. P. & Barbero, R. Global emergence of anthropogenic climate change in fire weather indices. *Geophys. Res. Lett.* **46**, 326–336 (2019).
- Bowman, D. M. et al. Vegetation fires in the Anthropocene. *Nat. Rev. Earth Environ.* **1**, 500–515 (2020).
- Boer, M. M., Resco de Dios, V. & Bradstock, R. A. Unprecedented burn area of Australian mega forest fires. *Nat. Clim. Change* **10**, 171–172 (2020).
- Shi, K. & Touge, Y. Characterization of global wildfire burned area spatiotemporal patterns and underlying climatic causes. *Sci. Rep.* **12**, 1–17 (2022).

8. Berna, F. et al. Microstratigraphic evidence of in situ fire in the Acheulean strata of Wonderwerk Cave, Northern Cape province, South Africa. *Proc. Natl Acad. Sci. USA* **109**, E1215–E1220 (2012).
9. Archibald, S., Staver, A. C. & Levin, S. A. Evolution of human-driven fire regimes in Africa. *Proc. Natl Acad. Sci. USA* **109**, 847–852 (2012).
10. Shimelmitz, R. et al. 'Fire at will': the emergence of habitual fire use 350,000 years ago. *J. Hum. Evol.* **77**, 196–203 (2014).
11. Paterson, A. Once were foragers: the archaeology of agrarian Australia and the fate of Aboriginal land management. *Quat. Int.* **489**, 4–16 (2018).
12. Huffman, M. R. The many elements of traditional fire knowledge: synthesis, classification, and aids to cross-cultural problem solving in fire-dependent systems around the world. *Ecol. Soc.* **18**, 3 (2013).
13. Ellis, E. C. et al. People have shaped most of terrestrial nature for at least 12,000 years. *Proc. Natl Acad. Sci. USA* **118**, e2023483118 (2021).
14. Fletcher, M. S., Hamilton, R., Dressler, W. & Palmer, L. Indigenous knowledge and the shackles of wilderness. *Proc. Natl Acad. Sci. USA* **118**, e2022218118 (2021).
15. Fletcher, M. S., Romano, A., Connor, S., Mariani, M. & Maezumi, S. Y. Catastrophic bushfires, indigenous fire knowledge and reframing science in Southeast Australia. *Fire* **4**, 61 (2021).
16. Hoffman, K. M. et al. Conservation of Earth's biodiversity is embedded in Indigenous fire stewardship. *Proc. Natl Acad. Sci. USA* **118**, e2105073118 (2021).
17. Roberts, P., Hunt, C., Arroyo-Kalin, M., Evans, D. & Boivin, N. The deep human prehistory of global tropical forests and its relevance for modern conservation. *Nat. Plants* **3**, 1–9 (2017).
18. Snitker, G. Identifying natural and anthropogenic drivers of prehistoric fire regimes through simulated charcoal records. *J. Archaeol. Sci.* **95**, 1–15 (2018).
19. Trauernicht, C., Brook, B. W., Murphy, B. P., Williamson, G. J. & Bowman, D. M. Local and global pyrogeographic evidence that indigenous fire management creates pyrodiversity. *Ecol. Evol.* **5**, 1908–1918 (2015).
20. Bush, M. B. et al. A palaeoecological perspective on the transformation of the tropical Andes by early human activity. *Phil. Trans. R. Soc. B* **377**, 20200497 (2022).
21. Stephens, L. et al. Archaeological assessment reveals Earth's early transformation through land use. *Science* **365**, 897–902 (2019).
22. Wurster, C. M. et al. Indigenous impacts on north Australian savanna fire regimes over the Holocene. *Sci. Rep.* **11**, 1–8 (2021).
23. Davies, B. et al. Fire and human management of late Holocene ecosystems in southern Africa. *Quat. Sci. Rev.* **289**, 107600 (2022).
24. Carter, V. A. et al. Legacies of Indigenous land use shaped past wildfire regimes in the Basin-Plateau Region, USA. *Commun. Earth Environ.* **2**, 1–9 (2021).
25. Archibald, S., Lehmann, C. E., Gómez-Dans, J. L. & Bradstock, R. A. Defining pyromes and global syndromes of fire regimes. *Proc. Natl Acad. Sci. USA* **110**, 6442–6447 (2013).
26. Abram, N. J. et al. Connections of climate change and variability to large and extreme forest fires in southeast Australia. *Commun. Earth Environ.* **2**, 1–17 (2021).
27. Nolan, R. H. et al. What do the Australian black summer fires signify for the global fire crisis? *Fire* **4**, 97 (2021).
28. Goergen, K., Lynch, A. H., Marshall, A. G. & Beringer, J. Impact of abrupt land cover changes by savanna fire on northern Australian climate. *J. Geophys. Res. Atmos.* **111**, 19106 (2006).
29. Bliege Bird, R., Bird, D. W., Coddling, B. F., Parker, C. H. & Jones, J. H. The 'fire stick farming' hypothesis: Australian Aboriginal foraging strategies, biodiversity, and anthropogenic fire mosaics. *Proc. Natl Acad. Sci. USA* **105**, 14796–14801 (2008).
30. Yibarbuk, D. et al. Fire ecology and Aboriginal land management in central Arnhem Land, northern Australia: a tradition of ecosystem management. *J. Biogeogr.* **28**, 325–343 (2001).
31. Scott, K. et al. Does long-term fire exclusion in an Australian tropical savanna result in a biome shift? A test using the reintroduction of fire. *Aust. Ecol.* **37**, 693–711 (2012).
32. Levick, S. R. et al. Rapid response of habitat structure and above-ground carbon storage to altered fire regimes in tropical savanna. *Biogeosciences* **16**, 1493–1503 (2019).
33. Murphy, B. P., Prior, L. D., Cochrane, M. A., Williamson, G. J. & Bowman, D. M. Biomass consumption by surface fires across Earth's most fire prone continent. *Glob. Change Biol.* **25**, 254–268 (2019).
34. Zupo, T., Gorgone-Barbosa, E., Ninno Rissi, M. & Daibes, L. F. Experimental burns in an open savanna: greater fuel loads result in hotter fires. *Austr. Ecol.* **47**, 1101–1112 (2022).
35. Woinarski, J. C. et al. Monitoring indicates rapid and severe decline of native small mammals in Kakadu National Park, northern Australia. *Wildl. Res.* **37**, 116–126 (2010).
36. Russell-Smith, J., Edwards, A. C., Sangha, K. K., Yates, C. P. & Gardener, M. R. Challenges for prescribed fire management in Australia's fire-prone rangelands—the example of the Northern Territory. *Int. J. Wildland Fire* **29**, 339–353 (2019).
37. Bowman, D. M. et al. Population collapse of a Gondwanan conifer follows the loss of Indigenous fire regimes in a northern Australian savanna. *Sci. Rep.* **12**, 1–17 (2022).
38. Lynch, A. H. et al. Using the paleorecord to evaluate climate and fire interactions in Australia. *Annu. Rev. Earth Planet. Sci.* **35**, 215–239 (2007).
39. Clarkson, C. et al. Human occupation of northern Australia by 65,000 years ago. *Nature* **547**, 306–310 (2017).
40. Bradshaw, C. J. A. et al. Stochastic models support rapid peopling of Late Pleistocene Sahul. *Nat. Commun.* **12**, 2440 (2021).
41. Bradshaw, C. J. A. et al. Directionally supervised cellular automaton for the initial peopling of Sahul. *Quat. Sci. Rev.* **303**, 107971 (2023).
42. Jones, R. Fire-stick farming. *Aust. Nat. Hist.* **16**, 224–228 (1969).
43. Kershaw, A. P. Climatic change and Aboriginal burning in north-east Australia during the last two glacial/interglacial cycles. *Nature* **322**, 47–49 (1986).
44. Mooney, S. D. et al. Late Quaternary fire regimes of Australasia. *Quat. Sci. Rev.* **30**, 28–46 (2011).
45. Williams, A. N., Mooney, S. D., Sisson, S. A. & Marlon, J. Exploring the relationship between Aboriginal population indices and fire in Australia over the last 20,000 years. *Palaeogeogr. Palaeoclimatol. Palaeoecol.* **432**, 49–57 (2015).
46. Rowe, C. et al. Holocene savanna dynamics in the seasonal tropics of northern Australia. *Rev. Palaeobot. Palynol.* **267**, 17–31 (2019).
47. Rowe, C. et al. Vegetation over the last glacial maximum at Gिरraween Lagoon, monsoonal northern Australia. *Quat. Res.* **102**, 39–52 (2021).
48. Hutley, L. B., Beringer, J., Isaac, P. R., Hacker, J. M. & Cernusak, L. A. A sub-continental scale living laboratory: spatial patterns of savanna vegetation over a rainfall gradient in northern Australia. *Agric. For. Meteorol.* **151**, 1417–1428 (2011).
49. Zhiseng, A. et al. Global monsoon dynamics and climate change. *Annu. Rev. Earth Planet. Sci.* **43**, 29–77 (2015).
50. Saiz, G. et al. Pyrogenic carbon from tropical savanna burning: production and stable isotope composition. *Biogeosciences* **12**, 1849–1863 (2015).
51. Bird, M. I. et al. Identifying the 'savanna' signature in lacustrine sediments in northern Australia. *Quat. Sci. Rev.* **203**, 233–247 (2019).
52. Rehn, E., Rowe, C., Ulm, S., Woodward, C. & Bird, M. A late-Holocene multiproxy fire record from a tropical savanna, eastern Arnhem Land, Northern Territory, Australia. *Holocene* **31**, 870–883 (2021).

53. Yang, F., Zhao, L., Gao, B., Xu, X. & Cao, X. The interfacial behaviour between biochar and soil minerals and its effect on biochar stability. *Environ. Sci. Technol.* **50**, 2264–2271 (2016).
54. Jing, F. et al. Interactions between biochar and clay minerals in changing biochar carbon stability. *Sci. Total Environ.* **809**, 151124 (2022).
55. Bradstock, R. A. A biogeographic model of fire regimes in Australia: current and future implications. *Glob. Ecol. Biogeogr.* **19**, 145–158 (2010).
56. Strickland, C., Liedloff, A. C., Cook, G. D., Dangelmayr, G. & Shipman, P. D. The role of water and fire in driving tree dynamics in Australian savannas. *J. Ecol.* **104**, 828–840 (2016).
57. Xu, X. et al. Tree cover shows strong sensitivity to precipitation variability across the global tropics. *Glob. Ecol. Biogeogr.* **27**, 450–460 (2018).
58. Bowman, D. M., Franklin, D. C., Price, O. F. & Brook, B. W. Land management affects grass biomass in the *Eucalyptus tetrodonta* savannas of monsoonal Australia. *Aust. Ecol.* **32**, 446–452 (2007).
59. Liedloff, A. C., Coughenour, M. B., Ludwig, J. A. & Dyer, R. Modelling the trade-off between fire and grazing in a tropical savanna landscape, northern Australia. *Environ. Int.* **27**, 173–180 (2001).
60. Prior, L. D. et al. Does inherent flammability of grass and litter fuels contribute to continental patterns of landscape fire activity? *J. Biogeogr.* **44**, 1225–1238 (2017).
61. Yates, C., MacDermott, H., Evans, J., Murphy, B. P. & Russell-Smith, J. Seasonal fine fuel and coarse woody debris dynamics in north Australian savannas. *Int. J. Wildland Fire* **29**, 1109–1119 (2020).
62. Murphy, B. P. & Russell-Smith, J. Fire severity in a northern Australian savanna landscape: the importance of time since previous fire. *Int. J. Wildland Fire* **19**, 46–51 (2010).
63. Perry, J. J. et al. Regional seasonality of fire size and fire weather conditions across Australia's northern savanna. *Int. J. Wildland Fire* **29**, 1–10 (2019).
64. Oliveira, S. L., Maier, S. W., Pereira, J. M. & Russell-Smith, J. Seasonal differences in fire activity and intensity in tropical savannas of northern Australia using satellite measurements of fire radiative power. *Int. J. Wildland Fire* **24**, 249–260 (2015).
65. Russell-Smith, J. et al. Managing fire regimes in north Australian savannas: applying Aboriginal approaches to contemporary global problems. *Front. Ecol. Environ.* **11**, e55–e63 (2013).
66. Whitehead, P. J., Bowman, D. M., Preece, N., Fraser, F. & Cooke, P. Customary use of fire by indigenous peoples in northern Australia: its contemporary role in savanna management. *Int. J. Wildland Fire* **12**, 415–425 (2003).
67. Kilinc, M. & Beringer, J. The spatial and temporal distribution of lightning strikes and their relationship with vegetation type, elevation, and fire scars in the Northern Territory. *J. Clim.* **20**, 1161–1173 (2007).
68. Saamak, C. F. A shift from natural to human-driven fire regime: implications for trace-gas emissions. *Holocene* **11**, 373–375 (2001).
69. Umbanhowar, C. E. & Mcgrath, M. J. Experimental production and analysis of microscopic charcoal from wood, leaves and grasses. *Holocene* **8**, 341–346 (1998).
70. Haliuc, A. et al. Microscopic charcoals in ocean sediments off Africa track past fire intensity from the continent. *Commun. Earth Environ.* **4**, 133 (2023).
71. Vachula, R. S. & Rehn, E. Modeled dispersal patterns for wood and grass charcoal are different: Implications for paleofire reconstruction. *Holocene* **33**, 159–166 (2023).
72. Murphy, B. P. et al. Using a demographic model to project the long-term effects of fire management on tree biomass in Australian savannas. *Ecol. Monogr.* **93**, e1564 (2023).
73. Lisiecki, L. E. & Stern, J. V. Regional and global benthic  $\delta^{18}\text{O}$  stacks for the last glacial cycle. *Paleoceanography* **31**, 1368–1394 (2016).

**Publisher's note** Springer Nature remains neutral with regard to jurisdictional claims in published maps and institutional affiliations.

**Open Access** This article is licensed under a Creative Commons Attribution 4.0 International License, which permits use, sharing, adaptation, distribution and reproduction in any medium or format, as long as you give appropriate credit to the original author(s) and the source, provide a link to the Creative Commons licence, and indicate if changes were made. The images or other third party material in this article are included in the article's Creative Commons licence, unless indicated otherwise in a credit line to the material. If material is not included in the article's Creative Commons licence and your intended use is not permitted by statutory regulation or exceeds the permitted use, you will need to obtain permission directly from the copyright holder. To view a copy of this licence, visit <http://creativecommons.org/licenses/by/4.0/>.

© The Author(s) 2024

## Methods

### Laboratory analyses

**Initial handling.** We split the core sections in half, and took samples of known volume at 5 or 10 cm intervals (depending on the changing nature of sediments) for pollen and micro-charcoal analysis and geochemistry (see below). We weighed, freeze-dried and reweighed samples to calculate the dry bulk densities.

**Pollen and PAR<sub>CHAR</sub>.** We processed 2 cm<sup>3</sup> sediment samples for pollen and micro-charcoal analysis. Sample preparation followed standard techniques<sup>74,75</sup>. We selected chemical preparations to disperse sedimentary materials initially, then progressively remove humic acids, calcium carbonates, bulk (in)organics and cellulose and silicates, as well as render pollen ornamentations more visible (including Na<sub>4</sub>P<sub>2</sub>O<sub>7</sub>, KOH, HCL, acetolysis and ethanol washes). We sieved at 125 µm and 7 µm. We added a *Lycopodium* spike during laboratory preparations to determine the relative concentrations of pollen and micro-charcoal particles.

We did pollen identifications at James Cook University based on regionally appropriate image and slide libraries built from collections at the lagoon and online resources such as the Australasian Pollen and Spore Atlas ([apsa.anu.edu.au](https://apsa.anu.edu.au)). Pollen sums averaged 300 grains. We present the proportion of total grass pollen as a percentage of total dryland pollen taxa in each sample, with the 97 taxa included in the dryland pollen sum detailed in Supplementary Table 2. The dryland pollen sum excludes all wetland-associated plant types, including riverine, floodplain, seasonal or permanent swamps, and lagoons of the Northern Territory. We also excluded spores identified as algal or Pteridophyte.

We counted micro-charcoal incorporated within the final pollen concentrate (black, opaque, angular particles >10 µm) simultaneously with pollen. We used the dry bulk density and the sedimentation rate derived from the age model (see below) to convert micro-charcoal particle counts to a PAR<sub>CHAR</sub>.

**MAR<sub>SPAC</sub> and δ<sup>13</sup>C<sub>SPAC</sub>.** We first decarbonated samples for TOC and SPAC, carbon isotope analysis and carbon isotope composition in 2 M HCl for 3 h. We isolated the SPAC component by hydrogen pyrolysis, now an established method for quantifying pyrogenic carbon<sup>76</sup>. We mixed approximately 250 mg of the sediment with a Mo catalyst using an aqueous methanol solution of ammonium dioxodithiomolybdate, sonicated and dried at 60 °C overnight. We placed the sample–catalyst mixture in a reactor, pressurized with H<sub>2</sub> to 150 bar with a purge gas flow of 5 l min<sup>-1</sup> and then heated at 300 °C min<sup>-1</sup> to 250 °C, and then at 8 °C min<sup>-1</sup> to 550 °C, which was held for 5 min. Labile carbon is removed during the hydrogen pyrolysis reaction, and the remaining carbon is composed of a stable form of pyrogenic carbon with more than seven condensed aromatic rings—this is defined as SPAC<sup>76</sup>.

We measured carbon abundance and carbon isotope composition by elemental analysis isotope ratio mass spectrometry using a ThermoScientific Flash EA with Smart EA option coupled with a ConFlo IV to a Delta VPlus at James Cook University's Advanced Analytical Centre. We determined carbon abundances using a thermal conductivity detector. We report carbon isotope measurements (in ‰) as deviations from the Vienna Pee Dee Belemnite (VPDB) reference standard scale for δ<sup>13</sup>C. We used USGS40 and two internal laboratory reference materials (Taipan, Chitin) within each analytical sequence for three-point calibrations of isotope delta-scale anchored by the VPDB. We calibrated our internal standards using USGS40 and USGS41 international reference materials and results have an uncertainty of ±0.2‰ or better. SPAC percentages have an average standard error of 2.2% of the value, which we corrected for possible in situ production of SPAC during the hydrogen pyrolysis reaction<sup>77,78</sup>. We used the dry bulk density and the sedimentation rate derived from the age model (see below) to convert SPAC abundances to MAR<sub>SPAC</sub>.

### Chronology

**Radiocarbon.** We pre-treated samples of bulk sediment for radiocarbon dating using hydrogen pyrolysis to remove labile carbon and decontaminate the charcoal component<sup>79</sup>. We combusted samples to CO<sub>2</sub> and reduced them to a graphite target for measurement at Australia's Nuclear Science and Technology Organisation<sup>79</sup>. Details of all radiocarbon dates used to construct the age model for the Girraween Lagoon record have been published previously<sup>46,47</sup>.

**Optically stimulated luminescence dating.** We extended the chronology for the sedimentary sequence at Girraween Lagoon beyond the limit of radiocarbon using optically stimulated luminescence dating. This method gives an estimate of the time since grains of quartz were last exposed to sunlight<sup>80</sup>. The time of sediment deposition is estimated by dividing the equivalent dose ( $D_e$ , the radiation energy absorbed by grains since deposition) by the environmental dose rate (the rate of supply of ionizing radiation to the grains since deposition).  $D_e$  is estimated from laboratory measurements of the optically stimulated luminescence from quartz. The environmental dose rate is estimated from laboratory measurements of environmental radioactivity, plus the small contribution from cosmic rays.

We collected 24 sediment samples from depths of between 467 and 1,670 cm below the present ground surface. We collected samples from one half of the split core in subdued red light. Each sample represents a 10 cm depth interval with the midpoint depth provided in Supplementary Table 1. We first removed light-exposed portions of the samples to measure the prevailing moisture content and radioactivity in the sediment to estimate the environmental dose rate. We then prepared the remaining light-safe core, and extracted quartz grains to measure the optically stimulated luminescence signal and estimate  $D_e$ .

We took single-grain optically stimulated luminescence measurements of  $D_e$  for all samples. We prepared and measured samples using methods and equipment described and tested previously<sup>81,82</sup>. We measured all single quartz grains with diameters of 180–212 µm using the single-aliquot regenerative dose procedure<sup>83,84</sup>. Aberrant grains were rejected using a standard set of quality assurance criteria<sup>81</sup>. We used two different methods (conventional single-aliquot regenerative dose and the weighted-mean natural signal ( $L_n T_n$ ) method<sup>85</sup>) to determine  $D_e$  for age estimates from the same data. We applied the  $L_n T_n$  method to samples that contained a large proportion of 'saturated' grains (that is, the optically sensitive traps filled with respect to dose), resulting in a truncation of their conventional single-aliquot regenerative dose  $D_e$  distributions and consequent underestimation of  $D_e$  and age<sup>82,86,87</sup>. We did all analyses for both methods using the functions implemented in R packages numOSL<sup>88,89</sup> and Luminescence<sup>90</sup>.

The environmental dose rate consists of the external beta, gamma and cosmic ray dose rates and an internal alpha dose rate. We assumed an internal alpha dose rate of  $0.031 \pm 0.008$  Gy kyr<sup>-1</sup> for all samples. We measured beta dose rates directly using a Risø GM-25-5 multi-counter system based on published procedures<sup>91–93</sup>. We calculated gamma dose rates from estimates of uranium (U) and thorium (Th) obtained from thick-source alpha counting and potassium (K) from inductively coupled plasma optical emission spectroscopy, except for two small organic-rich samples (GIR3-O-1992 and GIR3-R-1993), for which we measured the U, Th and K contents using instrumental neutron activation analysis. We converted the U, Th and K values to gamma dose rates (Gy kyr<sup>-1</sup>) using established dose rate conversion factors<sup>90</sup>. We also took into account the cosmic ray contribution to the total dose rate<sup>94</sup>, adjusting for site altitude (25.9 m), geomagnetic latitude and the density and thickness of water (1 m) and sediment (variable) overburden. We used an average density of water of 1.025 g cm<sup>-3</sup>. There is high variation in water content and bulk density of the sediment down-core. These differences in bulk density are important because energy loss per gram per cubic centimetre is greater at lower densities. We constructed a simple model assuming an average water depth of -1 m over the entire

burial period and used present-day sediment depths, moisture content and bulk density estimates.

We corrected the measured beta dose rates for grain-size attenuation, and adjusted the beta, gamma and cosmic ray dose rates for water content (based on the measured field values and bulk densities) and for organic attenuation for organic-rich samples<sup>95,96</sup>. We divided the sample  $D_e$  by the corresponding total environmental dose rates to calculate the optically stimulated luminescence ages in calendar years before present; the associated uncertainties are at the 68.2% confidence level and include all known and estimated sources of random and systematic error.

**Age model.** We applied a Bayesian approach for age modelling. We used the R package rbacon<sup>94</sup> to calibrate radiocarbon ages using the Southern Hemisphere calibration<sup>97</sup> SHCal20 and combined calibrated radiocarbon ages and optically stimulated luminescence ages for determination of depth probability distributions of age in R 4.0.0 (ref. 98). See Supplementary Fig. 4 for the age depth model and Supplementary Table 1 for the data associated with the new optically stimulated luminescence dates that we employed in generating the model. We used the mean output from the model. The average deviation of the median from the mean age at each increment across the whole record is 0.2% of the mean age, the maximum difference is 2.1% for ages older than 400 yr.

## Analysis

We hypothesized that the relationship between  $MAR_{SPAC}$  and  $PAR_{char}$  would shift with the onset of landscape-scale moderation of the fire regime by people. Under this hypothesis, the pre-human era would have higher-intensity fires and therefore more  $MAR_{SPAC}$  relative to  $PAR_{char}$  compared with the era dominated by anthropogenic fire regimes. This can be visualized as a bivariate plot of  $MAR_{SPAC}$  versus  $PAR_{char}$ , with the expectation that  $MAR_{SPAC}$  increases at a faster rate relative to  $PAR_{char}$  under the natural regime compared with the anthropogenic fire regime. Likewise, higher-intensity fires characteristic of natural fire regimes should produce lower  $\delta^{13}C_{SPAC}$  in charcoal given the higher preservation potential of coarse, woody fuels compared with fine, grassy fuels. We therefore expected a more pronounced positive relationship between the proportion of  $C_3$  to  $C_4$  biomass contributing to the char (as measured by  $\delta^{13}C_{SPAC}$ ) and the vegetation inferred from the percentage of grass pollen in total dryland pollen under an anthropogenic fire regime compared with a natural one.

We compared the relationship between  $MAR_{SPAC}$  and  $PAR_{char}$ , and between the percentage of grass pollen and  $\delta^{13}C_{SPAC}$ , in the definitive pre-human era with a period when humans had probably established landscape-scale fire control. Choosing the date of this transition is somewhat arbitrary because we do not know precisely when this human signal would have emerged, but this is immaterial for analysis given the necessity of testing the relationship only during periods of relatively wetter climates (as we explain below). Initially we chose 30 ka as the threshold date before which we assumed a natural fire regime, and after which an anthropogenic fire regime. Examining the bivariate relationships for these two periods while ignoring the relative wetness regime (as measured by TOC), there is little indication of a shift in the  $MAR_{SPAC}$  versus  $PAR_{char}$  and percentage of grass pollen versus  $\delta^{13}C_{SPAC}$  relationships as hypothesized; in fact, the slopes of the two relationships for the natural and anthropogenic fire regimes appear to be opposite to expectations (Supplementary Fig. 1). In the case of  $MAR_{SPAC}$  versus  $PAR_{char}$ , this is an artefact of the physical breakdown of micro-charcoal particles in the clay-rich sections of the core through the development of charcoal–mineral complexes such that the charcoal is comminuted into size classes finer than can be visually recognized (<10  $\mu m$ ) during laboratory disaggregation. We could identify the issue of comminution to finer particle sizes in our record because: (1) we had both clay-rich and clay-poor intervals to compare; and (2) we had a geochemical

measure of pyrogenic carbon abundance that did not rely on visually counting char particles in a particular size class.

When we considered the relationships through filtering by the TOC content such that we included only reliable  $PAR_{char}$  measurements, relationships emerged in the hypothesized direction: the trend for  $MAR_{SPAC}$  versus  $PAR_{char}$  was less pronounced under the natural fire regime, and the trend for the percentage of grass pollen versus  $\delta^{13}C_{SPAC}$  was more pronounced under the anthropogenic fire regime (Fig. 3).

To test whether such relationships were supported statistically, and to examine the sensitivity of the results to threshold choices (that is, minimum organic carbon abundance and the temporal transition point from natural to anthropogenic fire regimes), we implemented the following procedures. We first standardized the data to ensure that we had values at consistent and regular intervals along the time series using the ‘approx’ function in R; here, we took values every 250 years across each time series (that is, 150 ka, 145.75 ka, 145.50 ka ... 0 ka). This increment was a trade-off between uniform coverage of the time series and oversampling. The average temporal resolution across the entire record was 550 years.

Next, we split all of the time series at 30 ka; we assigned values >30 ka as the natural fire regime and values  $\leq$ 30 ka as the anthropogenic fire regime. We then filtered the time series to retain only the values by successively lower percentage TOC contents, starting with a threshold of >5.1% TOC, which was the lowest TOC percentage from 11 ka to the present (Fig. 1a). For the  $MAR_{SPAC}$  versus  $PAR_{char}$  relationship, we first  $\log_{10}$ -transformed each variable given the relationship’s power-law-like behaviour, and then randomly resampled  $x, y$  pairs (with replacement) from the natural-regime period using only the number of  $x, y$  pairs from the anthropogenic-regime period. Repeating this process 10,000 times, we calculated the number of iterations where the Spearman’s  $\rho$  for the resampled natural-regime relationship was less than Spearman’s  $\rho$  for the resampled anthropogenic-regime relationship. Dividing the number of times  $\rho_{natural} < \rho_{anthropogenic}$  by the number of iterations provided a probability that the observed difference in the relationships could be derived randomly (akin to a type I error probability). For the percentage of grass pollen versus  $\delta^{13}C_{SPAC}$  relationship, we applied the same process but instead calculated the numbers of times  $\rho_{natural} > \rho_{anthropogenic}$  to test the hypothesized change in the relationship.

To examine the sensitivity of the results to the choice of the TOC threshold, we repeated the procedure for both  $MAR_{SPAC}$  versus  $PAR_{char}$  and the percentage of grass pollen versus  $\delta^{13}C_{SPAC}$  for decreasing TOC (>10%, >9%, >8% ... >1%). To test the sensitivity of our results to the choice of the temporal threshold below and above which the categories of natural and anthropogenic fire regime applied, we repeated the resampling procedure at a wetness value of >5.1% TOC, but varied the temporal split by values of 1,000 yr either side of 30 ka to the extremes of 65 ka and 1 ka.

## Data availability

All data are available via GitHub at <https://github.com/cjabradshaw/FireRegimeShift>.

## Code availability

All code is available via GitHub at <https://github.com/cjabradshaw/FireRegimeShift>.

## References

- Bennett, K. D. & Willis, K. J. Pollen. In *Tracking Environmental Change Using Lake Sediments*, Vol. 3 (eds Smol, J. P. et al.) 5–32 (Springer, 2002).
- Brown, C. A. *Palynological Techniques* (American Association of Stratigraphic Palynologists, 2008).
- Wurster, C. M., Saiz, G., Schneider, M. P., Schmidt, M. W. & Bird, M. I. Quantifying pyrogenic carbon from thermosequences of wood and grass using hydrogen pyrolysis. *Org. Geochem.* **62**, 28–32 (2013).

77. Wurster, C. M., Lloyd, J., Goodrick, I., Saiz, G. & Bird, M. I. Quantifying the abundance and stable isotope composition of pyrogenic carbon using hydrogen pyrolysis. *Rapid Commun. Mass Spectrom.* **26**, 2690–2696 (2012).
78. Meredith, W., McBeath, A., Ascough, P. & Bird, M. I. in *Biochar: A Guide to Analytical Methods* (eds Singh, B. et al.) 187–198 (CRC, 2017).
79. Bird, M. I. et al. The efficiency of charcoal decontamination for radiocarbon dating by three pre-treatments – ABOX, ABA and hypy. *Quat. Geochronol.* **22**, 25–32 (2014).
80. Huntley, D. J., Godfrey-Smith, D. I. & Thewalt, M. L. Optical dating of sediments. *Nature* **313**, 105–107 (1985).
81. Jacobs, Z. et al. Timing of archaic hominin occupation of Denisova Cave in southern Siberia. *Nature* **565**, 594–599 (2019).
82. Forbes, M. et al. Comparing interglacials in eastern Australia: a multi-proxy investigation of a new sedimentary record. *Quat. Sci. Rev.* **252**, 106750 (2021).
83. Galbraith, R. F., Roberts, R. G., Laslett, G. M., Yoshida, H. & Olley, J. M. Optical dating of single and multiple grains of quartz from Jinmium rock shelter, northern Australia: part I, experimental design and statistical models. *Archaeometry* **41**, 339–364 (1999).
84. Murray, A. S. & Wintle, A. G. Luminescence dating of quartz using an improved single-aliquot regenerative-dose protocol. *Radiat. Meas.* **32**, 57–73 (2000).
85. Li, B., Jacobs, Z., Roberts, R. G., Galbraith, R. & Peng, J. Variability in quartz OSL signals caused by measurement uncertainties: problems and solutions. *Quat. Geochronol.* **41**, 11–25 (2017).
86. Li, B., Jacobs, Z. & Roberts, R. G. Validation of the LnTn method for De determination in optical dating of K-feldspar and quartz. *Quat. Geochronol.* **58**, 101066 (2020).
87. Fu, X. et al. Establishing standardised growth curves (SGCs) for OSL signals of individual quartz grains: a continental-scale case study. *Quat. Geochronol.* **60**, 101108 (2020).
88. Peng, J. & Li, B. Single-aliquot regenerative-dose (SAR) and standardised growth curve (SGC) equivalent dose determination in a batch model using the R package ‘numOSL’. *Anc. TL* **35**, 32–53 (2017).
89. Peng, J., Dong, Z. B., Han, F. Q., Long, H. & Liu, X. J. R package numOSL: numeric routines for optically stimulated luminescence dating. *Anc. TL* **31**, 41–48 (2013).
90. Kreutzer, S. et al. Introducing an R package for luminescence dating analysis. *Anc. TL* **30**, 1–8 (2012).
91. Bøtter-Jensen, L. & Mejdahl, V. Assessment of beta-dose-rate using a GM multicounter system. *Nucl. Tracks Radiat. Meas.* **14**, 187–191 (1988).
92. Jacobs, Z. & Roberts, R. G. An improved single grain OSL chronology for the sedimentary deposits from Diepkloof Rockshelter, Western Cape, South Africa. *J. Archaeol. Sci.* **63**, 175–192 (2015).
93. Guérin, G., Mercier, N. & Adamiec, G. Dose-rate conversion factors: update. *Anc. TL* **29**, 5–9 (2011).
94. Prescott, J. R. & Hutton, J. T. Cosmic-ray contributions to dose rates for luminescence and ESR dating: large depths and long-term time variations. *Radiat. Meas.* **23**, 497–500 (1994).
95. Lian, O. B., Hu, J. S., Huntley, D. J. & Hicock, S. R. Optical dating studies of Quaternary organic-rich sediments from southwestern British Columbia and northwestern Washington State. *Can. J. Earth Sci.* **32**, 1194–1207 (1995).
96. Blaauw, M. & Christen, J. A. Flexible paleoclimate age-depth models using an autoregressive gamma process. *Bayesian Anal.* **6**, 457–474 (2011).
97. Hogg, A. G. et al. SHCal20 Southern Hemisphere calibration, 0–55,000 years cal BP. *Radiocarbon* **62**, 759–778 (2020).
98. *R: A Language and Environment for Statistical Computing* (R Foundation for Statistical Computing, 2022).

## Acknowledgements

This work was funded by the Australian Research Council Centre of Excellence for Australian Biodiversity and Heritage (grant number CE170100015 to M.I.B., Z.J. and C.J.A.B.) and an Australian Research Council Laureate Fellowship (grant number FL140100044 to M.I.B.). We thank Larrakia Traditional Owners for permission to do this research on their traditional lands.

## Author contributions

M.I.B., C.M.W. and C.R. designed the study. M.I.B., C.M.W., C.R., M.B., R.C., X.H. and C.Z. undertook field sampling and laboratory analyses. Z.J. and X.F. performed the optically stimulated luminescence dating and C.J.A.B. conducted the statistical analyses. All authors contributed to the interpretation. M.I.B. wrote the manuscript and all authors contributed to the final form of the manuscript.

## Competing interests

The authors declare no competing interests.

## Additional information

**Supplementary information** The online version contains supplementary material available at <https://doi.org/10.1038/s41561-024-01388-3>.

**Correspondence and requests for materials** should be addressed to Michael I. Bird.

**Peer review information** *Nature Geoscience* thanks Grant Snitker, Nicholas O’Mara and the other, anonymous, reviewer(s) for their contribution to the peer review of this work. Primary Handling Editor: James Super, in collaboration with the *Nature Geoscience* team.

**Reprints and permissions information** is available at [www.nature.com/reprints](http://www.nature.com/reprints).